Applied Catalysis B: Environmental 88 (2009) 576–581

Contents lists available at ScienceDirect

Applied Catalysis B: Environmental

journal homepage: www.elsevier.com/locate/apcatb

Visible-light-induced photocatalytic inactivation of bacteria by composite photocatalysts of palladium oxide and nitrogen-doped titanium oxide

Pinggui Wu [a,*], Rongcai Xie [a], James A. Imlay [b], Jian Ku Shang [a]

[a] Department of Materials Science and Engineering, University of Illinois at Urbana-Champaign, 1304 W. Green St., Urbana, IL 61801, USA
[b] Department of Microbiology, University of Illinois at Urbana-Champaign, Urbana, IL 61801, USA

ARTICLE INFO

Article history:
Received 18 September 2008
Received in revised form 24 November 2008
Accepted 9 December 2008
Available online 27 December 2008

Keywords:
Titanium oxide
Photocatalyst
Photocatalysis
Composite
Water
Disinfection

ABSTRACT

Composite photocatalysts of palladium oxide and nitrogen-doped titanium oxide (PdO/TiON) were synthesized by a sol–gel process, as convenient forms of nanopowder or immobilized powder on nanofiber. The PdO/TiON catalysts were tested for visible-light-activated photocatalysis using different bacterial indicators, including gram-negative cells of *Escherichia coli* and *Pseudomonas aeruginosa*, and gram-positive cells of *Staphylococcus aureus*. Disinfection data indicated that PdO/TiON composite photocatalysts have a much better photocatalytic activity than either palladium-doped (PdO/TiO_2) or nitrogen-doped titanium oxide (TiON) under visible-light illumination. The roles of Pd and N were discussed in terms of the production and separation of the charge carriers under visible-light illumination. The photocatalytic activity was thus dependent on dopants and light intensity. Microscopic characterization demonstrated that visible-light photocatalysis on PdO/TiON caused drastic damage on the bacteria cell wall and the cell membrane.

1. Introduction

Titanium dioxide has been extensively studied as a photocatalyst for energy conversion [1–3] and environmental application [3–8] since the discovery of its photoelectrochemical effect by Fujishima and Honda [9]. Photocatalytic inactivation of microorganisms upon TiO_2 under ultraviolet (UV) irradiation was first demonstrated by Matsunaga et al. [6]. Since then, various microbial organisms have been inactivated upon UV/TiO_2 [7,8,10–14]. However, pure TiO_2 photocatalyst requires UV irradiation for activation due to its wide band gap of 3.2 eV in the TiO_2 anatase crystalline phase [3]. This requirement has limited the use of TiO_2 photocatalysis because of the small UV portion (~5%) in the solar spectrum. To address the problem, much effort has been devoted to the development of visible-light-activated photocatalysts by doping TiO_2 with either transition metals [15,16] or nonmetal anions [17–29]. Since Asahi et al. [17] reported the visible-light photo-activity of TiO_2 with nitrogen doping, many groups have demonstrated that anion doping of TiO_2 extends the optical absorbance of TiO_2 into the visible-light region. The reported anionic dopants include N [18–25], C [26], S [27], F [28], and P [29]. Anionic doping provides advantages of dopant stability and ease of the doping process. However, the photocatalytic activity of these doped materials was rather low owing to a low quantum yield under visible light activation [25].

Recently, codoping approaches have shown that a second element confers a synergistic sensitizing effect to anion-doped TiO_2, thereby enhancing visible-light-induced photo-activity [30–32]. Our group has recently reported enhanced visible-light photoactivity of palladium-modified nitrogen-doped TiO_2. We first discovered that PdO nanoparticles in a PdO/TiON thin film can be reduced to metallic palladium under visible-light illumination [33], which may reduce electron–hole recombination rate during photocatalysis and enhance the visible-light photo-activity. Later, we synthesized PdO/TiON nanopowders by a sol–gel process and demonstrated their enhanced photocatalytic activity over TiON in degradation of humic acid [34]. Despite the development of effective visible-light-induced photocatalysts in our group and other groups, there have been only a limited number of reports on metal ion and anion co-doped TiO_2. The study of antimicrobial properties and environmental applications of (cation and anion) co-doped TiO_2 is apparently missing.

In this article, we synthesized (Pd, N)-doped TiO_2 nanopowder photocatalysts and embedded the resultant PdO/TiON nanopowder onto a fiber matrix, which renders a convenient form for application. The objective of this communication is to provide a broad investigation on the bactericidal kinetics of these PdO/TiON materials under visible-light irradiation. We found

* Corresponding author.
E-mail addresses: pwu1@uiuc.edu (P. Wu), jkshang@uiuc.edu (J.K. Shang).

0926-3373/$ – see front matter © 2008 Elsevier B.V. All rights reserved.
doi:10.1016/j.apcatb.2008.12.019

that visible-light illumination of the PdO/TiON photocatalysts completely inactivated both gram-negative and gram-positive bacteria in <50 min.

2. Experimental

2.1. Materials and synthesis

A previous report on PdO/TiON nanopowder detailed how the photocatalyst was prepared, and the preparation of immobilized PdO/TiON followed the same sol–gel ingredients [34]. Activated carbon-coated glass fiber (ACGF) [35,36] was kindly provided by Prof. James Economy at the University of Illinois at Urbana-Champaign. The ACGF as received has a surface area of 650–750 m^2/g. Pieces of ACGF were soaked in the precursor mixture for 24 h at room temperature. After wash and dry, fine crystallites of PdO/TiON were obtained by 3 h calcination at 400 °C in air, followed by removal of carbon at 500 °C in air for 1 h. Single element doped photocatalysts PdO/TiO_2 and TiON were made in the same method. In a comparison study to verify that palladium ion itself is not bactericidal, PdO incorporated in an inert matrix of SiO_2, i.e., the PdO/SiO_2 powder, was also synthesized by a former method [37] using tetraethyl-orthosilicate (TEOS) as the silica precursor.

2.2. Photocatalyst characterizations

To obtain morphological information, photocatalysts immobilized in the fiber form were observed using a JEOL JSM-7000F analytical scanning electron microscope (JEOL Ltd., Tokyo, Japan) operated at 15 kV. The immobilized amount of TiON/PdO nanoparticles on the ACGF after calcination was estimated from inductively coupled plasma (ICP) elemental analysis of the titanium element with OES Optima 2000 DV (PerkinElmer, Norwalk, CT, USA).

2.3. Cell culture and viability assay

Bacterial strains and the corresponding media used in this study at the Department of Microbiology, University of Illinois at Urbana-Champaign, are listed in Table 1. The cells were grown aerobically in the medium placed on a rotary shaker at 30 or 37 °C for 18 h. Cells were harvested from the overnight culture by centrifugation, washed twice using a buffer solution (0.05 M KH_2PO_4 and 0.05 M K_2HPO_4, pH 7.0), then resuspended and diluted in buffer prior to the use for sterilizing experiments. The initial cell concentration was controlled to the magnitude of 10^7 colony-forming units per ml (cfu/ml), as determined by a viable count procedure on agar plates after serial dilutions. All solid or liquid materials have been autoclaved for 30 min at 121 °C before use.

The experimental set-up for a static bactericidal testing is shown schematically in Fig. 1, where a bacterial solution mixed with a photocatalyst is illuminated by a visible light source. At starting time (t_0), 3-ml aliquots of bacterial suspension were pipetted onto a sterile 60 mm × 15 mm petri dish. A proper amount of powder or fiber-cut was soaked completely in the cell suspension to make a desirable catalyst concentration, which was a default 1.0 g/L or as stated. The covered petri dishes were illuminated by a metal halogen desk lamp which blocks UV irradiation with its built-in glass filter. The light intensity below 400 nm was <0.01 mW/cm^2. The visible-light intensity striking the cells were adjusted based on the distance of the petri dish lid from the lamp, measured center-point by a Multi-Sense™ MS-100 optical radiometer (UVP Inc., Upland, CA) at 1.6 mW/cm^2 or as stated. The temperature of the cell suspension increased from room temperature to a maximum 40 °C under illumination. Cell suspension was continuously stirred for the beginning 5 min and then was stirred periodically during irradiation, especially for 1 min prior to every aliquot-withdrawal.

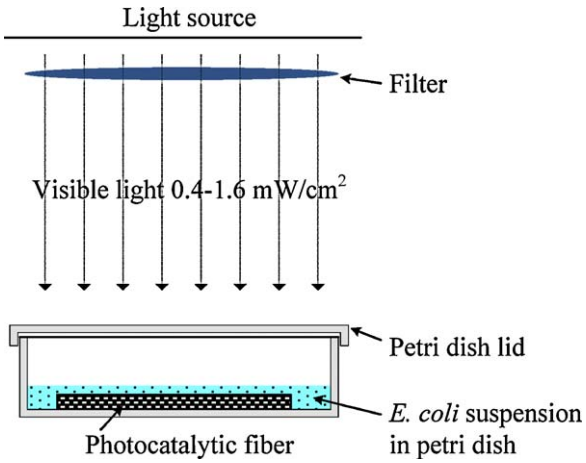

Fig. 1. Schematic illustration of the photocatalytic testing setup.

At regular time intervals, 20-μl (1.0 ml for the last time point) aliquots of the irradiated cell suspension were withdrawn. After appropriate dilutions in buffer solution, a 20-μl aliquot together with 2.5 ml top agar was spread onto an agar medium plate and incubated at 37 °C for 24 h. See Fig. S1, Supporting Information, for a demonstration of the viable count method with colonies of bacteria on medium plates. A survival ratio is determined as $N(t)/N(t_0)$, with N being the number of viable cells in colony-forming units. The data and conclusions were confirmed by replicate experiments (typical variation within ±10%). Control runs were carried out without photocatalysts in the cell suspension. Cell viability on irradiated blank ACGF matrix was also tested. Comparison was made via parallel tests, if ever possible.

2.4. Electron microscopy of E. coli cells

For a preliminary mechanistic study on the photocatalytic disinfection, overnight grown *Escherichia coli* cell culture at 10^9–10^{10} cfu/ml before and after photocatalytic treatment were collected by centrifugation. The pellet was fixed in 2.5% glutaraldehyde for 2 h in a refrigerator. After fixation, the cell pellets were soaked in cacodylate buffer to remove excess fixative.

Table 1
Strains and media composition (per liter) used.

	E. coli AN387, wild-type [40]	*P. aeruginosa* ATCC 10145	*S. aureus* ATCC 25923
Liquid medium (pH 7.0)	LB: 10 g bactotryptone; 5 g yeast extract; 10 g NaCl	Difco nutrient broth (NB): 5 g beef extract; 3 g peptone	BACTO tryptic soy broth (TSB): 17 g pancreatic digest of casein; 3 g enzymatic digest of soybean; 2.5 g dextrose; 5.0 g NaCl; 2.5 g K_2HPO_4
Plate	Liquid medium + additional 15 g bactoagar		
Top agar	Liquid medium + additional 8 g bactoagar		

Post-fixation processing was carried out in 1% osmium tetroxide in cacodylate buffer for 90 min at room temperature, and the pellets were then washed with cacodylate buffer. The samples were dehydrated by a successive soakings in 37, 67 and 95% (v/v) ethanol for 10 min each, and three soakings in 100% ethanol for 15 min each. Critical point drying was performed by placing samples in hexamethyldisilazane (HMDS) for 45 min and let dry overnight under a fume hood, after drawing the HMDS off. SEM images of the samples were obtained using a scanning electron microscope Hitachi S-4700 (Hitachi, Tokyo, Japan) at an acceleration voltage 5 or 10 kV.

3. Results and discussion

3.1. Characterization of PdO/TiON

Basic compositional, structural, optical, and morphological characteristics of PdO/TiON nanopowder were reported previously and will not be reiterated [34,38,39]. Table 2 provides a summary of these characteristics. After the PdO/TiON nanoparticles were immobilized on the fiber matrix support, the PdO/TiON was found to retain anatase crystalline phase in XRD, and similar chemical composition of Pd_{3d}, Ti_{2p}, N_{1s} and O_{1s} in XPS. Thus, the optical property of the embedded PdO/TiON powder would remain similar to that of the reported PdO/TiON powders [34]. As indicated in our previous data of XRD, XPS, and scanning transmission electron microscopy (STEM) of PdO/TiON fiber materials, the palladium additive is present as PdO not incorporated into the dominant crystalline structure of nitrogen-doped TiO_2 [38,39]. The weight percentage of immobilized amount of PdO/TiON nanoparticles on the ACGF after calcination, calculated based on ICP elemental analysis, is about 2.5 wt.%. Fig. 2 shows representative SEM images of the PdO/TiON powder-immobilized fiber sample. The initial ACGF template contained interconnected nano-sized pores (*ca.* 2 nm) in the activated carbon. The nano-pores of carbon were filled with the PdO/TiON precursor. Upon crystallization, the fiber consisted of a composite structure in which carbon and PdO/TiON nanoparticles were intertwined. The PdO/TiON powder-immobilized ACGF fiber photocatalysts exhibit bi-modal porous characteristics after calcination. Firstly, removal of the carbon template upon calcination resulted in a nanoporous structure of the interconnected PdO/TiON particles. Secondly, the initial fiber support has a large pore skeleton. SEM image Fig. 2a shows the opening of nonwoven fabric fibers, tens to hundreds of micrometers in dimension. These large pores are desirable both for improving the contact efficiency between the bacterial cells and the photocatalyst, and for reducing the pressure drop across the fabric in a dynamic reactor. Fig. 2b shows the immobilization of PdO/TiON particles on the fiber support. The surface area of powder-immobilized ACGF remains to be in the range 650–750 m^2/g.

3.2. Effect of doping

E. coli is a widely used bacteria indicator in photocatalytic tests. Owing to its easy growth and non-toxicity, wild-type *E. coli* AN387

Table 2
Properties of PdO/TiON nanoparticles in powder and fiber samples.

	PdO/TiON in powder [34]	PdO/TiON in fiber
Crystalline phase	Pure anatase	Pure anatase
Composition	Existence of N, O, Pd, and Ti	Existence of N, O, Pd, and Ti (Fig. S2, Supporting Information)
Optical property	Higher visible-light absorption than TiON (>400 nm)	Same as in powder
Crystalline size	20–25 nm (by XRD)	Not determined

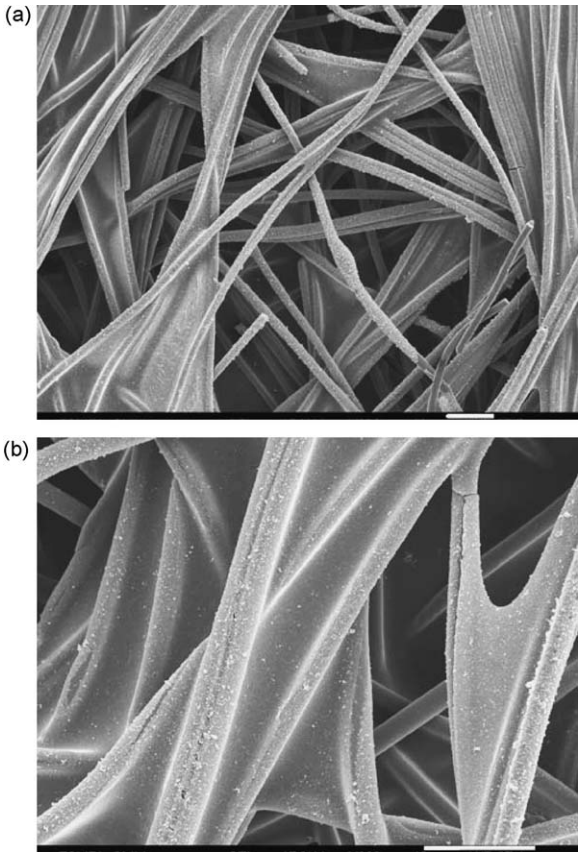

Fig. 2. Scanning electron microscopy images of immobilized PdO/TiON powder on ACGF fiber matrix. The scale bar shown at the bottom of each image is 30 μm. The difference between (a) and (b) is solely the magnification.

[40] was used here for a few comparative studies. In investigating the antimicrobial property of PdO/TiON photocatalysts, we first determined how the PdO, the PdO/TiO_2 and PdO/TiON affected the photosterilization. For this purpose, PdO/SiO_2, PdO/TiO_2 and PdO/TiON nanopowders with the same Pd/Si or Pd/Ti atomic ratio at 0.5% in sol–gel precursors were made and tested for *E. coli* disinfection at 1.0 g/L in suspension. Results in Fig. 3 show that PdO/TiON is superior to PdO/SiO_2 or PdO/TiO_2 in terms of the photo-activity under visible light. First of all, PdO by itself on an inert SiO_2 substrate does not offer significant bactericidal effect.

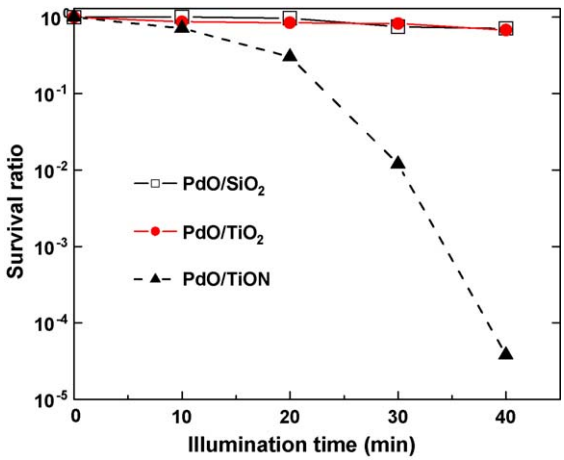

Fig. 3. Survival of *E. coli* on PdO/SiO_2, PdO/TiO_2 and PdO/TiON powder samples under visible-light illumination 1.6 mW/cm^2. Control data (not drawn) form a nearly overlapping flat line with those of PdO/TiO_2.

Secondly, addition of PdO in the TiO_2 does not generate noticeable bactericidal action under visible-light irradiation either. This is not surprising since it has been previously reported that the optical absorption edge of PdO/TiO_2 does not have much shift to the visible light regime [33]. Thirdly, PdO/TiON powders possess a red-shift to the visible light regime owing to the nitrogen doping in the TiO_2 lattice (Table 2), and the small amount of incorporated PdO acted as electron traps to separate oppositely charged electrons and holes, resulting in greater photocatalytic efficiency. It was noted that the Pd additive can also promote visible-light absorption in nitrogen-doped TiO_2 [34]. The visible light absorption is essential to the charge production on the semiconductor photocatalyst. Such dual roles of PdO significantly enhanced the photocatalytic activity of PdO/TiON under visible-light illumination.

Similar finding with regard to the significance of PdO was confirmed with the testing of powder-immobilized fiber photocatalysts. In Fig. 4, sterilization tests indicated that the undoped TiO_2-immobilized fibers virtually have no bactericidal effect under visible-light illumination, forming a horizontal line that is almost overlapping with the control test (i.e., irradiation without photocatalysts). On the contrary, the bactericidal function of TiON-immobilized fiber became more and more evident with longer illumination time. An overall trend of gradual decrease in the survival ratio was observed for *E. coli* cells treated by TiON-immobilized fibers, achieving *ca.* 60% killing after an hour. This reduction magnitude is in agreement with the sulfur-doped titanium oxide for bacteria inactivation reported by Yu et al. [27]. Apparently nitrogen doping has enabled photocatalytic sterilization without the use of UV light; however, the killing rate was low. With PdO/TiON in Fig. 4, sterilization was greatly accelerated, reaching a survival ratio $<10^{-5}$ by 25 min of irradiation at 1.6 mW/cm^2. In 30 min, the cells survived $<10^{-7}$ which was beyond detection limit. It can also be seen that the survival curve of *E. coli* is first order. There is a shoulder for the beginning 0–10 min, which corresponds to the initial lag phase that is often observed in photo-disinfection responses. After the shoulder period, the inactivation rate increases considerably. The fastest disinfection occurred during the next 10–30 min of illumination.

The observed difference in killing rate of PdO/TiON toward *E. coli* in Figs. 3 and 4 may be attributed to the way powder was stirred and dispersed. Non-stop stirring is more desirable to increase the killing rate of PdO/TiON powder in Fig. 3.

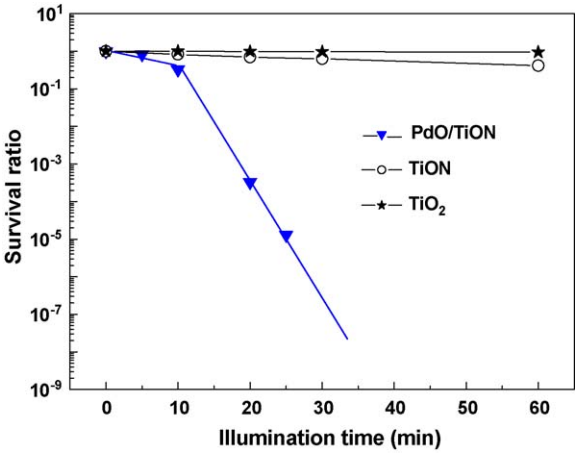

Fig. 4. Survival of *E. coli* on TiO_2, TiON and PdO/TiON powder-immobilized fiber samples under visible-light illumination 1.6 mW/cm^2. At 30 min upon the PdO/TiON, survival $< 10^{-7}$. Control data (not drawn) form a nearly overlapping flat line with those of TiO_2.

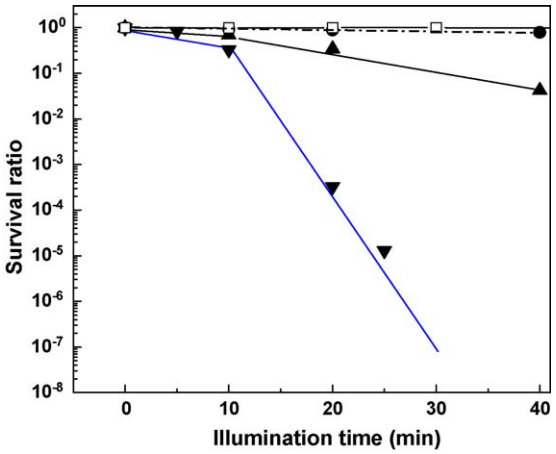

Fig. 5. Effect of visible-light intensity on the photocatalytic inactivation of *E. coli* by PdO/TiON-immobilized fiber: in the dark (dash line, ●), 0.4 mW/cm^2 (▲), and 1.6 mW/cm^2 (▼), respectively. Control data (without fiber) are shown in open square.

3.3. Effect of light intensity

As shown in Fig. 5, the intensity of illumination was found to influence the bactericidal effect strongly. With other conditions being equal, when the intensity of visible light was decreased from about 1.6 mW/cm^2 to about 0.4 mW/cm^2, the killing rate declined significantly. The survival ratio was still 4% after 40 min of irradiation at 0.4 mW/cm^2. The associated change of suspension temperature is minimal, thus the reduction in disinfection rate is likely due to the slower kinetics that are normally expected in a photochemical reaction when the irradiance is reduced. In the dark condition, PdO/TiON-immobilized fiber did not initiate the bactericidal effect. In the meantime, our test on pieces of original ACGF (without PdO/TiON particles) does not show reduction in bacteria counts over time (data not presented).

3.4. Inactivation of pathogens

Besides *E. coli*, the PdO/TiON photocatalysts were tested toward two types of pathogenic bacteria including both gram-negative and gram-positive strains. *Pseudomonas aeruginosa* ATCC 10145 cells were chosen as one of the indicators because of their significance as human pathogens. These bacteria are ubiquitous in nature and create persistent opportunistic infections, aided by their ability to form biofilms that can oppose host clearance mechanisms. The bacteria are also difficult to treat medicinally, as they elaborate several antibiotic-resistance systems [41].

The effect of the photocatalyst on the viability of *P. aeruginosa* cells was studied by exposing the cells suspended in buffer solution to a visible light for varying time intervals. We have previously reported the bactericidal effect of TiON-immobilized fiber on *P. aeruginosa* cells [36]. Fig. 6a shows that TiON treatment resulted in a survival ratio of 57% upon 30 min illumination and 32% upon 60 min illumination. The effect of the co-doped photocatalyst PdO/TiON on the viability of *P. aeruginosa* cells was more drastic in Fig. 6a. A steep curve of inactivation was observed for *P. aeruginosa* cells treated by PdO/TiON-immobilized fibers, with *ca.* 10^{-6} surviving at 20 min illumination, and $<10^{-7}$ survival ratio at 30 min. The beneficial effect of Pd ion and N doping in TiO_2 was again demonstrated on the inactivation of *P. aeruginosa* cells.

A similar killing trend was observed in Fig. 6b for the inactivation of the gram-positive bacterium *Staphylococcus aureus*. Although the inactivation of *S. aureus* was a little slower, the pseudo-first order of the killing curve is comparable to the

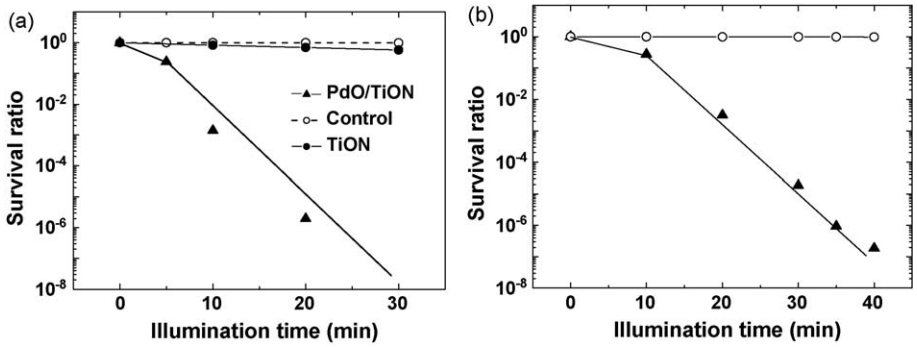

Fig. 6. (a) Survival of *P. aeruginosa* on TiON and PdO/TiON-immobilized fiber samples; at 30 min upon the PdO/TiON, survival $< 10^{-7}$. (b) Survival of *S. aureus* on PdO/TiON-immobilized fiber (▲), vs. control (○) without photocatalysts. Visible-light illumination was 1.6 mW/cm^2 in both (a) and (b).

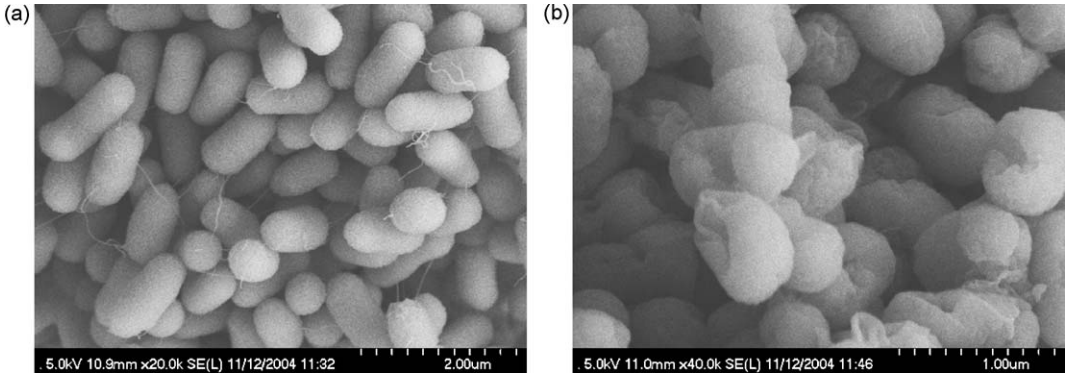

Fig. 7. SEM images of *E. coli* cells (a) prior to and (b) after photocatalytic treatment upon PdO/TiON disinfection.

inactivation of gram-negative cells *E. coli* and *P. aeruginosa*. The small difference of inactivation time may be due to the variation in cell-envelope structure, but more work would need to be done with other bacteria strains to test this correlation. Our studies on these different strains of bacteria demonstrate that PdO/TiON effectively inactivate both gram-negative and gram-positive bacteria.

3.5. Evidence of cell damage

Scanning electron microscopy (SEM) has been used as a suitable method for investigation of cell morphology. SEM was used to study the biocidal action and mechanism of the PdO/TiON photocatalyst. Fig. 7a illustrates a representative SEM image of *E. coli* cells irradiated without using photocatalyst. In this control, the surfaces of rod-like bacteria are continuous and damage-free. It indicates that the cells were healthy. However, after complete inactivation of the *E. coli* cells upon illumination in the presence of PdO/TiON photocatalyst, the morphologies of cells have drastic changes. First, flagella which were observed in Fig. 7a of untreated cells were completely missing in Fig. 7b of photocatalytically treated cells. Second, in nearly every cell the appearance of rumples and high degree of disordered configurations were observed after treatment. Fig. 7b shows that many *E. coli* cells had mass-missing on the cell wall and the cell membrane or further inside, which developed as deep 'holes'. These results showed that treated cells with PdO/TiON particles were damaged, forming pits and holes in their cell walls. The possible killing mechanisms are yet to be established. However, on the UV-activated TiO_2, photocatalytic killing has been linked to the membrane damage by oxidative radicals [42–44] and to loss of metabolic activities [42]. Both hydroxyl radicals and superoxide have been suggested as the working species [42,45]. Results from our preliminary study suggest that similar mechanisms appear to operate in the visible-light illumination of PdO/TiON photocatalysts [46]. Those results will be discussed in a subsequent report.

Although a direct comparison between the photocatalytic efficiency of PdO/TiON and the other reported activity of doped or undoped TiO_2 is not possible due to the lack of standardized conditions, it shall be noted that the survival fraction $<10^{-5}$ within *ca.* 30 min is one of the fastest rates in photocatalytic disinfection of *E. coli*. For most of the data reported using TiO_2 under UV to inactivate *E. coli*, either a longer illumination time was required to achieve survival ratio $<10^{-5}$ or higher survival ratio was still remained after 30 min [6,14,42,47,48]. The visible-light photosterilization efficiency as reported previously is even lower [27,31,36,49]. There are few studies on photocatalytic inactivation of *S. aureus*. Only a few reports [50,51] have dealt with *P. aeruginosa* cells using TiO_2 under UV irradiation. Based on its antimicrobial characteristics, PdO/TiON material is a strong visible-light photocatalyst for sterilization and environmental applications.

Acknowledgements

We thank Prof. J. Economy and Prof. Z. Yue for donation of ACGF fiber template. Financial support for this study was provided by the Center of Advanced Materials for the Purification of Water with Systems, National Science Foundation, under Grant No. CTS-0120978. Characterization of fiber was carried out at the Frederick Seitz Materials Research Laboratory, University of Illinois at Urbana-Champaign, which is partially supported by U.S. Department of Energy under grant DEFG02-91-ER45439.

Appendix A. Supplementary data

Supplementary data associated with this article can be found, in the online version, at doi:10.1016/j.apcatb.2008.12.019.

References

[1] S. Khan, M. Al-Shahry, W. Ingler, Science 297 (2002) 2243–2245.
[2] B.O.R.M. Gratzel, Nature 353 (1991) 737–740.
[3] M.R. Hoffmann, S.T. Martin, W. Choi, D.W. Bahnemann, Chem. Rev. 95 (1995) 69–96.
[4] P.C. Zhang, R.J. Scrudato, G. Germano, Chemosphere 28 (1994) 607–611.
[5] F.M. Salih, J. Appl. Microbiol. 92 (2002) 920–926.
[6] T. Matsunaga, T.R. Tomoda, T. Nakajima, H. Wake, FEMS Microbiol. Lett. 29 (1985) 211–214.
[7] P.S.M. Dunlop, J.A. Byrne, N. Manga, B.R. Eggins, J. Photochem. Photobiol. A 148 (2002) 355–363.
[8] E.J. Wolfrum, J. Huang, D.M. Blake, P.C. Maness, Z. Huang, J. Fiest, W.A. Jacoby, Environ. Sci. Technol. 36 (2002) 3412–3419.
[9] A. Fujishima, K. Honda, Nature 238 (1972) 37–38.
[10] P.A. Christensen, T.P. Curtis, T.A. Egerton, S.A.M. Kosa, J.R. Tinlin, Appl. Catal. B: Environ. 41 (2003) 371–386.
[11] K. Sunada, T. Watanabe, K. Hashimoto, Environ. Sci. Technol. 37 (2003) 4785–4789.
[12] A. Vohra, D.Y. Goswami, D.A. Deshpande, S.S. Block, J. Ind. Microbiol. 32 (2005) 364–370.
[13] R.J. Watts, S.H. Kong, M.P. Orr, G.C. Miller, B.E. Henry, Water Res. 29 (1995) 95–100.
[14] M. Cho, H.M. Chung, W.Y. Choi, J.Y. Yoon, Appl. Environ. Microbiol. 71 (2005) 270–275.
[15] M. Iwasaki, M. Hara, H. Kawada, H. Tada, S. Ito, J. Colloid Interface Sci. 224 (2000) 202–204.
[16] M.I. Litter, Appl. Catal. B: Environ. 23 (1999) 89–114.
[17] R. Asahi, T. Morikawa, T. Ohwaki, K. Aoki, K. Taga, Science 293 (2001) 269–271.
[18] S.W. Yang, L. Gao, J. Am. Ceram. Soc. 87 (2004) 1803–1805.
[19] H. Irie, Y. Watanabe, K. Hashimoto, J. Phys. Chem. B 107 (2003) 5483–5486.
[20] J.L. Gole, J.D. Stout, C. Burda, Y.B. Lou, X.B. Chen, J. Phys. Chem. B 108 (2004) 1230–1240.
[21] C. Burda, Y. Lou, X. Chen, A.C.S. Samia, J. Stout, J.L. Gole, Nano Lett. 3 (2003) 1049–1051.
[22] P.G. Wu, C.H. Ma, J.K. Shang, J. Appl. Phys. A 81 (2005) 1411–1417.
[23] S. Sakthivel, M. Janczarek, H. Kisch, J. Phys. Chem. B 108 (2004) 19384–19387.
[24] M. Mrowetz, W. Balcerski, A.J. Colussi, M.R. Hoffman, J. Phys. Chem. B 108 (2004) 17269–17273.
[25] M. Miyauchi, A. Ikezawa, H. Tobimatsu, H. Irie, K. Hashimoto, Phys. Chem. Chem. Phys. 6 (2004) 865–870.
[26] Y.Z. Li, D.S. Hwang, N.H. Lee, S.J. Kim, Chem. Phys. Lett. 404 (2005) 25–29.
[27] J.C. Yu, W.K. Ho, J.G. Yu, H. Yip, P.K. Wong, J.C. Zhao, Environ. Sci. Technol. 39 (2005) 1175–1179.
[28] J.C. Yu, J.G. Yu, W.K. Ho, Z.T. Jiang, L.Z. Zhang, Chem. Mater. 14 (2002) 3808–3816.
[29] L. Lin, W. Lin, Y.X. Zhu, B.Y. Zhao, Y.C. Xie, Chem. Lett. 34 (2005) 284–285.
[30] H. Liu, L. Gao, J. Am. Ceram. Soc. 87 (2004) 1582–1584.
[31] Q. Li, R.C. Xie, Y.W. Li, E.A. Mintz, J.K. Shang, Environ. Sci. Technol. 41 (2007) 5050–5056.
[32] Y. Sakatani, H. Ando, K. Okusako, H. Koike, J. Nunoshige, T. Takata, J.N. Kondo, M. Hara, K. Domen, J. Mater. Res. 19 (2004) 2100–2108.
[33] Q. Li, W. Liang, J.K. Shang, Appl. Phys. Lett. 90 (2007) 063103–063109.
[34] Q. Li, R. Xie, E.A. Mintz, J.K. Shang, J. Am. Ceram. Soc. 90 (2007) 3863–3868.
[35] Z. Yue, C.L. Mangun, J. Economy, Carbon 40 (2002) 1181–1191.
[36] P.G. Wu, R. Xie, J. Imlay, J.K. Shang, in: A. Wereszczak, E. Lara-Curzio, M. Mizuno (Eds.), Advances in Bioceramics and Biocomposites II, Ceramic Eng. Sci. Proc., Wiley-American Ceramic Society, 2006, pp. 125–128.
[37] C.T. Kresge, M.E. Leonowicz, W.J. Roth, J.C. Vartuli, J.S. Beck, Nature 359 (1992) 710–712.
[38] P. Wu, R. Xie, J.K. Shang, J. Am. Ceram. Soc. 91 (2008) 2957–2962.
[39] Q. Li, L.Y. W, P. Wu, R. Xie, J.K. Shang, Adv. Mater. 20 (2008) 3717–3723.
[40] S. Korshunov, J.A. Imlay, J. Bacteriol. 188 (2006) 6326–6334.
[41] B.R. Boles, M. Thoendel, P.K. Singh, Proc. Natl. Acad. Sci. U.S.A. 101 (2004) 16630–16635.
[42] D.M. Blake, P.C. Maness, Z. Huang, E.J. Wolfrum, J. Huang, W.A. Jacoby, Sep. Purif. Methods 28 (1999) 1–50.
[43] Z.X. Lu, L. Zhou, Z.L. Zhang, W.L. Shi, Z.X. Xie, H.Y. Xie, D.W. Pang, P. Shen, Langmuir 19 (2003) 8765–8768.
[44] J. Kiwi, V. Nadtochenko, Langmuir 21 (2005) 4631–4641.
[45] Y. Koizumi, R. Yamada, M. Nishioka, Y. Matsumura, T. Tsuchido, M. Taya, J. Chem. Technol. Biotechnol. 77 (2002) 671–677.
[46] P.-G. Wu, Antimicrobial materials for water disinfection based on visible-light photocatalysts, Mater. Sci. Eng., Ph.D. Dissertation, University of Illinois, Urbana-Champaign, 2007, p. 212.
[47] S.K. Devipriya, R. Yesodharan, Pollut. Res. 24 (2005) 89–91.
[48] J.C. Ireland, P. Klostermann, E.W. Rice, R.M. Clark, Appl. Environ. Microbiol. 59 (1993) 1668–1670.
[49] P.G. Wu, J.K. Shang, Materials Research Society (MRS) Symposium Proceeding of 2006 Spring Symposium JJ: Materials Science of Water Purification, San Francisco, California, U.S.A., April 2006, vol. 930E, ID JJ02-10, October 2006.
[50] O. Seven, B. Dindar, S. Aydemir, D. Metin, M.A. Ozinel, S. Icli, J. Photochem. Photobiol. A 165 (2004) 103–107.
[51] J. Robertson, P. Robertson, L. Lawton, J. Photochem. Photobiol. A 175 (2005) 51–56.